JOURNAL OF MATERIALS SCIENCE 31 (1996) 3589–3596

Polymer–clay nanocomposites: Free-radical grafting of polystyrene on to organophilic montmorillonite interlayers

A. AKELAH*
Chemistry Department, Tanta University, Tanta, Egypt
A. MOET
Macromolecular Science Department, Case Western Reserve University, Cleveland, OH 44106, USA

Vinyl monomer–montmorillonite intercalates, which are able to swell and disperse in organic solvents, have been prepared by a cation exchange process by the interaction between the Na^+ or Ca^{2+} cations of montmorillonite and vinylbenzyltrimethylammonium chloride. The resulting vinyl monomer–montmorillonite materials have been identified by X-ray diffraction (XRD), elemental analysis and infrared absorption spectra. Free-radical solution polymerizations of the penetrated styrene between the interlayers of 5, 10, 25 and 50 wt% vinyl monomer–montmorillonite have resulted in grafted polystyrene–montmorillonite materials. The effect of montmorillonite amounts on the formed polystyrene was determined by extraction with organic solvents, which showed an increase in the grafted polymer formed (0.84–2.94 g/g MMT), and a decrease in the external polystyrene with increasing amounts of montmorillonite. The molecular weight of the external polystyrenes was found to be in the range of 22 000. The vinyl monomer–montmorillonite and polymer–montmorillonite intercalates have been identified by XRD, elemental analysis and infrared spectroscopy. Examination of the polystyrene–montmorillonite materials by SEM, TEM and XRD showed spherical particles of nanosize about 150–400 nm, and basal spacings of 1.72–2.45 nm.

1. Introduction

Normally it is difficult to produce structural engineering polymers that combine both high strength and high toughness. High strength is a reflection of the ability of a material to sustain high loads, whereas high toughness involves a material for which a large amount of energy is absorbed during fracture. Fracture in a polymer occurs by the breaking of primary (covalent) and/or secondary (van der Waals or hydrogen-) bonds, depending upon the structure of the polymer. Improvements of the lack of toughness shown by brittle polymers have taken place particularly by the incorporation of rubbers through blending or copolymerization, whereas inorganic materials have been used to improve the strength of the polymers. However, there is still a significant need to produce polymers with extremely high levels of strength and toughness properties, in order for them to become widely accepted as structural engineering materials.

Polymer–clay materials have received considerable interest because the interactions between them have effects on the properties of both clay and polymer systems [1, 2]. Clays have been extensively used in the polymer industry either as reinforcing agents to improve the physico-mechanical properties of the final polymers or as fillers to reduce the amount of the polymers used in shaped structures, i.e. to act as diluents for the polymer, thereby lowering the uneconomically high cost of the polymer systems. The efficiency of the clay to modify the properties of the polymer is primarily determined by the degree of its dispersion in the polymer matrix which, in turn, depends on the clay particle size. However, the hydrophilic nature of the clay surfaces impedes their homogeneous dispersion in the organic polymer phase.

Some attempts have been made to prepare the polymer–clay materials. The impregnation technique of the clay by a vinyl monomer such as tetrafluoroethylene [3], *cis*- and *trans*-butene-2 [4], butadiene, 4-vinylpyridine [5] acrylamide [5], methyl methacrylate [6, 7], acrylonitrile [8–10], and styrene [11], followed by their polymerization, has been used for these cases by using a free-radical initiator. However, because the adsorption of monomer molecules between the lamellae depends on the dipole moment of the monomer molecule, the yields of the physically inserted polymer

---

*Present address: Chemistry Department, Faculty of Science, UAE University, P.O. Box 17551, Al-Ain, United Arab Emirates.

0022-2461

were found to be low. In addition, transformations of clay to azo–clay [12, 13] and vinyl–clay through isocyanate interaction [14] or lead exchange [15, 16] have been employed to prepare polymer–clay materials. These transformations have not led to a change in the hydrophilic nature of the clay to one with organophilic properties. The incompatibility of the clay layers in the organic monomer phase impedes their homogeneous dispersion and results in surface modification of the clays. The only way that leads to the penetration of the polymer to the interlayer space of the modified clay, is the condensation polymerization of caprolactam in the presence of clay–aminolauric, or clay–aminocaproic acid intercalates to give a nylon 6-clay hybrid [17–20].

The direct adsorption of uncharged linear polymers such as poly(vinylalcohol) [21], poly(vinylpyrrolidone) [22], poly(ethylene glycol) [23], and polyacrylamide [24], on to a clay surface has been used for preparing polymer–clay materials depending on the desorption of the hydration water molecules from surfaces. Because the entropy thus gained provides the driving force for this physical adsorption, it does not lead to high polymer adsorption, as the enthalpy change of the process is commonly very small. In some other cases, the polymers have been grafted to the available hydroxyl groups on the clay surface through coupling agents, which contain two reactive groups, one suitable for reaction with the polymer and the other capable of reacting with the clay [25, 26]. However, such surface modification processes to improve the properties of the clays with the polymers do not lead to penetration of the polymers between the interlayers of the clay, and hence they are not mutually homogeneously dispersed.

In a preliminary article [27], we reported the ability of the penetrated styrene between the swelled montmorillonite interlayers to polymerize, producing organophilic polystyrene–montmorillonite through chemical bonds. The objective of the present work was directed towards a complete study of the grafted polystyrene on montmorillonite interlayers by determining the structural composition and characteristics of these novel organic–inorganic nanocomposite materials.

2. Experimental procedure

2.1. Materials

Montmorillonite (MMT) minerals were supplied by ECC America Inc. under the trade names Meniral Colloid-BP for Na–MMT and Bentolite-L for Ca–MMT. The Na–MMT was received as fine particles with an average particle size of 75 μm, cation exchange capacity (CEC) of 90 mEq/100 g and interlayer spacings of 0.96 nm. The Ca–MMT was obtained as very fine particle with average size of 15 μm and CEC of 80 mEq/100 g. The minerals were purified by dispersion in distilled water and allowed to stand for several hours to allow settling of quartz sand and heavy materials. The suspensions were decanted and treated with 0.1 M aqueous solution of NaCl. The mixtures were filtered, followed by repeated washing with deionized water and filtration until no chloride ions were detected in the filtrates by reaction with $AgNO_3$ solution. The washed MMT materials were vacuum dried at 250 °C.

TABLE I Characteristics of vinyl monomer–MMT intercalates

No.	M	Analysis			(mmol[a]/ 100 g)	XRD	
		C (%)	H (%)	N (%)		*d* (nm)	Δ*d*(nm)
IIa	Na	9.96	1.70	0.86	108.20	15	5.4
IIb	Ca	9.83	1.41	0.66	83.20	14.9	5.3

[a] According to the N%.

Vinylbenzyltrimethyl ammonium chloride (VBTMAC, I) was prepared by the reaction of a mixture of *m*- and *p*-chloromethylstyrene (m : p ratio was ~ 30%: 60%, and 10% ethylstyrene Polyscience) with Me_3N according to the procedure previously described in the literature [28–30]. The crude product was purified through a filtration column using neutral alumina as a support and a 1 : 3 ether–MeCN mixture as eluent.

2.2. Vinyl monomer–montmorillonite intercalates (II)

A suspension of 25 g prewashed Na- or Ca–MMT in 1 l water was stirred overnight. To the stirred, cooled (0–5 °C), suspension, an aqueous solution of 30 mmol VBTMAC, I, in 100 ml water was added dropwise. After stirring for 3 h at 0–5 °C, the white precipitate was filtered, washed with water, methanol and ether, and dried in vacuum at room temperature to give 29.5 g IIa. The composition of the intercalated VBTMA cations in MMT layers and the spacing of silicate layers are shown in Table I.

2.3. Polystyrene–montmorillonite materials (III)

In a 500 ml three-necked flask, fitted with a condenser and a nitrogen inlet tube, 2.5 g VM–MMT (IIa) and 100 ml solvent were added and stirred under nitrogen for 1 h. To the stirred suspension, 50 ml styrene and 0.1 g AIBN were added. The mixture was then heated at 80 °C under stirring for 5 h. After cooling, the product was precipitated by the addition of the colloidal suspension to methanol. The precipitated PS–MMT hybrid was filtered, washed with methanol, and dried in vacuum at 100 °C. The polymerization solvents and characteristics of the resulting PS–MMT materials are listed in Table II.

2.4. Material characterization

The properties and structural characteristics of the vinyl monomer–montmorillonite and polystyrene–montmorillonite materials were identified by several techniques. Analyses of the elements carbon, hydrogen and nitrogen for II and III materials were carried out at Galbraith Lab Inc., and the results of their loadings are shown in Tables I and III For infrared measurements, approximately 2% of the sample was added to KBr and pressed into pellets. The sample pellets were then run on a Digilab FTS-14 FTIR, from 4000–600 (cm^{-1}) wave numbers.

TABLE II Preparation conditions and characteristics of PS–MMT materials

PS–MMT no.	IIa (wt %)	Polym. Solv. (ml/100 g)	XRD[a]		DSC T_g
			d (nm)	Δd (nm)	
IIIa	5	MeCN (40) + Tol (60)	2.03	1.07	81
IIIb	10	MeCN (125)	2.45	1.49	90.5
IIIc	10	MeCN (125) + THF (125)	2.22	1.26	94
IIId	25	MeCN (200) + Tol (200)	1.81	0.84	100
IIIe	50	MeCN (400) + Tol (400)	1.72	0.76	95.2

[a] Δd = (spacing of VM–MMT or MMT–PS − 0.96 nm).

TABLE III Characteristics of the extracted PS–MMT materials

PS–MMT no.	Ext. PS (wt %)	Int. PS–MMT				MMT (wt %)	Int PS (wt %)	Int PS/1/g MMT
		(wt %)	C(%)	H(%)	XRD (nm)			
IIIa	80.31	19.69	54.14	5.25	2.29/1.12	25.4	74.6	2.94
IIIb	78.91	21.09	25.88	2.86	2.17	47.4	52.6	1.11
IIIc	74.91	25.09	31.96	3.55	1.89	39.8	60.2	1.51
IIId	42.26	57.74	23.00	2.90	1.71/1.01	43.3	56.7	1.31
IIIe	10.49	89.51	16.28	2.51	2.08/1.06	55.9	44.1	0.84

X-ray powder diffraction (XRD) data on powdered samples of all II and III materials were determined by an autodiffractometer which consisted of a Phillips XRG 3100 X-ray generator equipped with a nickel-filtered CuK$_\alpha$ ($\lambda = 1.541\,80$ nm) as the X-ray source, and connected to a Phillips APD 3520 type PW 1710 diffractometer controller. The scanning speed was 0.005° (2θ) s^{-1}. Bragg's Law, $\lambda = 2d \sin\theta$, was used to compute the crystallographic spacing, d.

The morphology of the polystyrene–montmorillonite materials was examined by SEM and TEM. A Jeol JSM-353F scanning electron microscope, set at an electron voltage of 25 kV, was used for high-magnification observations of PS–MMT particles. The thin-film specimens for transmission electron microscopy (TEM) were prepared by immersing the TEM grid in suspensions of PS–MMT materials in tetrahydrofuran (THF, 0.5%), and then dried at room temperature followed by heating at 50 °C under vacuum to ensure complete solvent removal.

Differential scanning calorimetry (DSC) of all PS–MMT materials was performed on a Perkin–Elmer DSC 7 differential scanning calorimeter. The glass transition temperatures, T_g of the polystyrenes were determined from the respective DSC thermograms.

2.5. Measurement of molecular weights of extracted polystyrenes

The crude powdered PS–MMT material (3 g) was stirred overnight at room temperature in 75 ml toluene. The colloidal aggregates were centrifuged and the supernatant liquid separated by decantation. This procedure was repeated many times using THF, acetone and DMF as extraction solvents, until no more polymer was found in the supernatant liquid. The solution that contains the extractable polystyrene, was poured into methanol to recover the external polystyrene, which is then dried and weighed. The solvent-extracted PS–MMT product was washed with MeOH, vacuum dried and weighed. The extracted polystyrene fractions were dissolved in toluene and the solutions were used to determine the viscosity average molecular weight at 30 °C. The analyses and characteristics of the extractable polystyrene and extracted PS–MMT materials are listed in Table III.

2.6. Water-uptake measurements

Compression-moulded samples (23 mm × 3 mm × 1 mm) were prepared at 215.5 °C, 10 metric ton, for 0.15 h using a Carver Lab Press. Each specimen was weighed, then dried in a vacuum oven at 60 °C overnight. After redetermining the weight of the dried specimens, they were immersed in distilled water and 0.4 M aqueous NaCl solution at room temperature for a month, at the end of which the water uptake was determined. The characteristic properties of the pressure-moulded PS–MMT materials are listed in Table IV.

TABLE IV Characteristics of moulded PS–MMT materials

PS–MMT no.	XRD (nm)	Water uptake (%)	
		Moisture	Aq. NaCl
IIIa	20	0.23	0.26
IIIb	20	0.25	0.40
IIId	14.6	0.94	1.88

3. Results and discussion

The goal of our research is directed towards producing polymer–clay composites which can exhibit the characteristic properties of the individual components, i.e. the high strength and toughness combination. This objective can be attained by inducing specific chemical interactions between the polymer and the smectitic clay interlayers. This, in turn, requires a change in the chemical and physical properties of the clay in order to render it an organophilic character. The chemical grafting of polymers on to montmorillonite interlayers was achieved either by polymerization or by chemical modification techniques.

Montmorillonite (MMT) is a hydrous alumino-silicate mineral composed of units made up of two silica tetrahedral sheets with a central alumina octahedral sheet, so that the oxygen ions of the octahedral sheet also belong to the tetrahedral sheets [31–33]. From electron microscopy [34, 35], the MMT mineral is basically composed of aggregates, whose size often ranges between 0.1 and 10 μm: that are made up by association of a number of primary particles (structural units) which, in turn, are composed of a number of superimposed lamellae. The height of the primary particle is 8–10 nm, its diameter is 30 nm, and its thickness is 0.96–1.0 nm. Thus, each primary particle contains approximately 8 lamellae or 16 (0 0 1) planes.

In the present work, the chemical grafting of polystyrene (PS) on to MMT interlayers by the addition polymerization technique was achieved in two stages. The first stage included the preparation of vinyl monomer–MMT intercalate by a cation exchange process between a compound containing ammonium and vinyl groups (VM) that are capable of forming bonds with the negative charges of the MMT interlayers and with the formed polystyrene. The second stage included the free-radical polymerization of styrene in the presence of different ratios of VM–MMT intercalate (5%, 10%, 25% and 50%) to yield PS–MMT materials as shown in Fig. 1. Such mutual charge neutralization results in a marked increase of the organophilic property of the VM–MMT that leads to the attraction and penetration of styrene molecules and hence swelling of the clay prior to the onset of polymerization. The marked reduction in the water affinity of VM–MMT intercalates (IIa, b) has facilitated their separation and washing with polar solvents.

The cation exchange capacity (CEC) of Na- and Ca–MMT with the ions of vinyl monomer was determined from the elemental analyses of the nitrogen content

$$\mathrm{CEC} = [c_{\mathrm{N}} \times 1000]/[(14 \times n_{\mathrm{N}}/\mathrm{MW}) \times 100] \quad \mathrm{mmol/100\ g\ MMT} \qquad (1)$$

where C_{N} is the content of nitrogen (wt %), and n_{N} the number of nitrogen atoms of the cation. Thus, the total exchange capacities for IIa and IIb were 108.2 mmol Amm ion/100 g and 83.2 mmol Amm ion/100 g silicate skeleton. However, IIa and IIb contain 61.43 mmol N/100 g and 47.14 mmol N/100 g silicate, as calculated from

$$\mathrm{Loading} = [c_{\mathrm{N}} \times 1000]/[14 \times n_{\mathrm{N}}] \quad \mathrm{mmol\ N/100\ g\ MMT} \qquad (2)$$

Infrared spectra of the VM–MMT complex, IIa (Fig. 2a) shows the characteristic bands corresponding to the ammonium salt and their methyl groups. The $-\mathrm{N^+Me_3}$ groups gave adsorption at about 3450 $\mathrm{cm^{-1}}$, corresponding to the C–H stretching vibrations of the $\mathrm{CH_3}$ group, and at 1500 $\mathrm{cm^{-1}}$, corresponding to the $\mathrm{N^+Me_3}$ vibrations.

The basal spacing of VM–MMT intercalate IIa was determined to be 1.5 nm. Because the basal spacing of the dried MMT without any adsorbed cations or water equals about 0.96 nm, the vinyl monomer layer thickness would amount to about 0.54 nm. The basal spacing of IIb was found to be 1.49 nm and the thickness of the vinyl monomer layer was about 0.53 nm, which is similar to that of IIa.

On the basis of the swelling characteristic of the VM–MMT derivative, IIa, in the organic solvents that results in strong separation of the interlayers, the solution polymerization technique is used in this study for the preparation of PS–MMT materials. The use of a suitable solvent to promote and maximize the swelling of the VM–MMT interlayers is primarily due to solvation of the interlayer cations, which is considered to be a result of a balance between the interlayer cohesive forces and the attractive force required to increase the interlayer distance. Thus, the role of the solvents, which have strong attractive forces to the

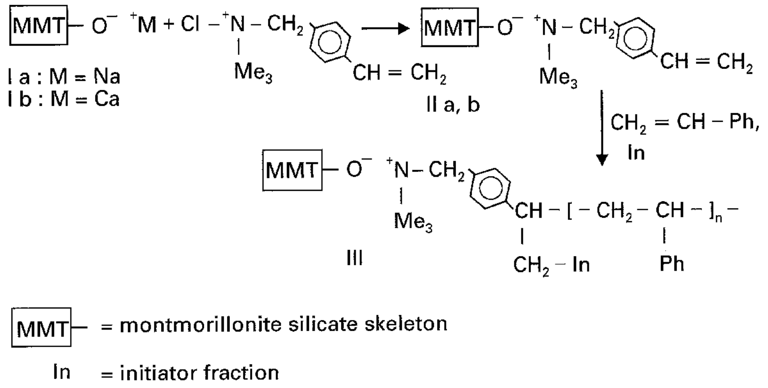

Figure 1 Preparation of vinyl monomer–MMT intercalates and their free-radical polymerizations with styrene.

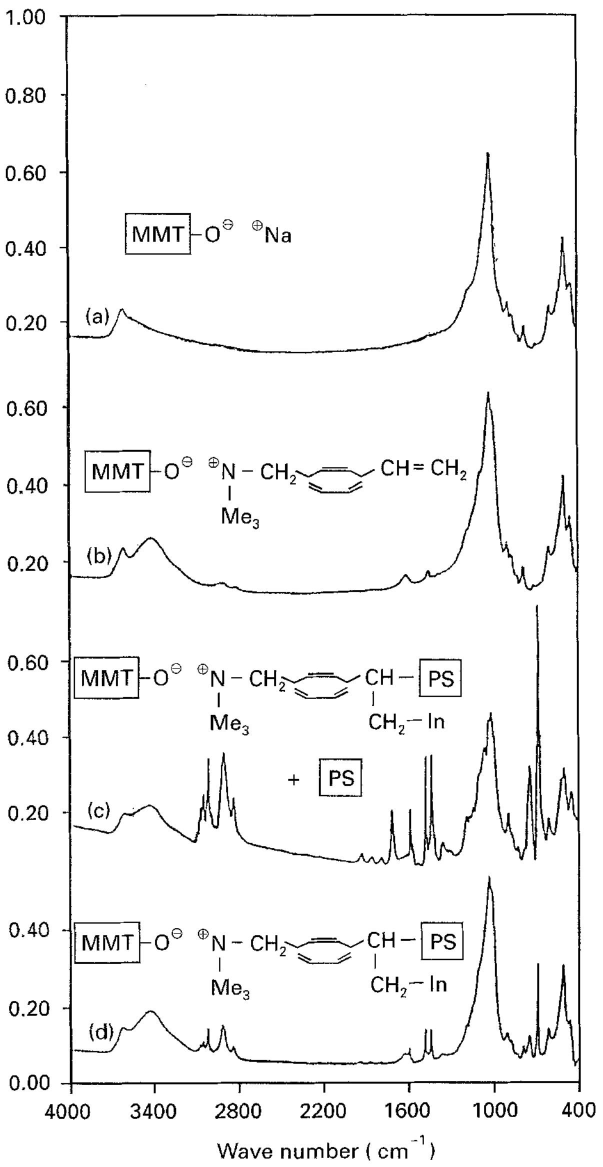

Figure 2 Infrared spectra of (a) Na–MMT, (b) vinyl monomer–MMT intercalate, IIa, (c) crude PS–MMT material, III, (d) extracted PS–MMT material.

VM–MMT intercalate, is to improve wetting of the MMT layers and to stimulate penetration of the styrene between the wetted layers. The efficiency of this nature depends on the type of solvent used. For example, the solvation of VBTMA–MMT intercalate with acetonitrile, appears to have facilitated the movement and inclusion of styrene molecules between the VM–MMT layers prior to the onset of polymerization and hence led to PS–MMT material with a basal spacing of 2.45 nm. This significant penetration of styrene is perhaps attributed to the high dipole moment of the MeCN which appears to have caused the high association in the liquid state.

Because acetonitrile is a good solvent for styrene but a poor solvent for PS, the solvation of VM–MMT intercalate has also been carried out with a mixture of MeCN/THF, and MeCN/toluene. In these mixtures, MeCN assists the swelling of VM–MMT intercalate and hence facilitates the penetration of styrene molecules between the lamellae. THF and toluene, on the other hand, impart a degree of flexibility to the MMT–PS propagating chain for assisting further insertion of styrene molecules during the polymerization process. Although the mixtures have facilitated the penetration of the styrene between the lamellae as indicated by the changes in basal spacing of the products, the increase in the interlayer distance was less than that associated with MeCN.

The basal spacing expansion summarized in Table II suggests that interlayer accessibility to styrene molecules is related to the solvation energy of the used solvent mixture. Presumably, polymerization was initiated in the interlayer region and once the polymerization started, the MMT–PS propagating chains were swollen by the styrene molecules because of the sufficiently attractive force between styrene and the interlayer polystyrene propagating chains. Accordingly, the effect of the initial amount of styrene monomer inserted between the interlayers before the onset of polymerization is the main factor causing the increase in the intercalation of PS molecules between the interlayers. On the other hand, the mobility of the propagating polystyrene chains which are confined between the lamellae is certainly restricted on using a mixed solvent when compared to the mobility of propagating PS chains in MeCN. The basal spacing of PS–MMT material amounted 2.45 nm, hence the thickness of PS layers in between the lamellae reached 1.49 nm in the case of MeCN. However, when mixed solvents are used, the thickness of the polystyrene layers reached lower values, as shown in Table II. The infrared absorption spectrum of the washed PS–MMT materials (Fig. 2b, c) showed the characteristic bands due to CH stretching (3025 cm^{-1}), C–C skeletal in-plane vibration (1600 1495, 1455 cm^{-1}), and CH out-of-plane deformation (755, 690 cm^{-1}).

Even though the polymerization is designed to produce polystyrene that is grafted to the interlayer of MMT, the probability of polymerization outside the clay particles is probably equal. The extraction of non-grafted polystyrene from the PS–MMT materials was carried out to differentiate between the grafted polystyrene, which results from polymerization of the interlamellae penetrated styrene monomer, and external PS, which results from the polymerization of the styrene around the MMT aggregates. Although toluene as a non-polar solvent has extracted all of the non-grafted polystyrene, acetone and DMF, as aprotic solvents, were also used for extracting any residual adsorbed polystyrene. From the results of the extraction shown in Table III, it appears that the amount of PS grafted into MMT interlayers strongly depends on the conditions of polymerization and on the initial amount of styrene monomer penetrated in the interlayer space of the VM–MMT intercalate, which increased with increasing MMT content. This separation technique has led to a study of the effect of MMT ratios on the molecular weight of the external PS and the ratio of the formed PS to MMT, through the determination of the molecular weights of the extractable PS from their intrinsic viscosities at different concentrations in toluene. The determined molecular weight is in the range of 22 000 ($a = 0.72$, $K = 9.2 \times 10^{-3}$ ml g^{-1}) and remains fairly constant throughout the various polymerizations that occur under different circumstances. Apparently, the molecular weight of the external polystyrene is smaller than those of common polystyrenes and depends on the presence of MMT, which may lead to chain-transfer termination of the propagating polystyrene chains.

The composition of the crude PS–MMT material, i.e. the per cent conversion of styrene to grafted (non-extractable) and homo-PS (extractable) and the ratio of the grafted-PS to the MMT, were calculated from the weights of the crude PS–MMT material, extractable PS and extracted PS–MMT material. The quantities of the grafted PS were confirmed by calcination at 1000 °C of the sample previously extracted and dried to constant weight. The results listed in Table III indicate that the formation of homo-PS is greatly decreased while the formation of grafted-PS is increased by increasing the available MMT layers. In addition, the ratios of the grafted-PS to MMT significantly decreased on increasing the amount of MMT in PS–MMT materials. However, the two values for the interlamellar spacings obtained for some of the extracted PS–MMT materials, shown in Table III, are attributed to the presence of more than one interlamellar spacing within the sample, i.e. a part is expanded and the other is less expanded.

In order to study the effect of MMT ratios on the molecular mobility of PS chains and hence on the T_g of the formed PS, DSC curves for PS–MMT materials have been determined, as listed in Table II. The range of values indicates that the PS obtained is of a relatively high molecular weight. However, the extracted polystyrenes have molecular weights of 22 000, as determined from their intrinsic viscosities. This means that the MMT has a chain-transfer termination effect on the formed PS chains.

Examination of the PS–MMT materials by optical microscopy has shown the effect of polystyrene compositions on the morphology of the modified MMT materials. Investigation of the microstructure of the PS–MMT intercalate, IIIb, prepared from IIa without using swelling solvent in the polymerization mixture, by SEM (Fig. 4) indicates the non-separation of the MMT interlayers. However, investigation of the microstructure of the PS–MMT intercalate, IIIb, prepared by swelling IIa in the solvent and monomer mixture before polymerization, by SEM (Fig. 5) shows that the particle size is below the resolution of the SEM. The transmission electron micrograph in Fig. 6 shows that the MMT–PS intercalates have spherical particles of size about 150–400 nm in diameter. When the PS–MMT materials are pressure moulded under the conditions of 215.5 °C and 10 metric ton for 0.15 h, the scanning electron micrograph in Fig. 7 shows no microscopic voids. This indicates that the MMT components of these materials do not agglomerate, and retain their integrity after moulding. This non-agglomeration tendency of MMT particles is an indication for the possibility of their utilization in the compounding formulations to improve the properties of the mixed polymer matrices. The transmission electron micrograph of Fig. 6 also indicates that the PS–MMT material is actually a mixture of homo-PS and spherical particles with a good particle–matrix adhesion.

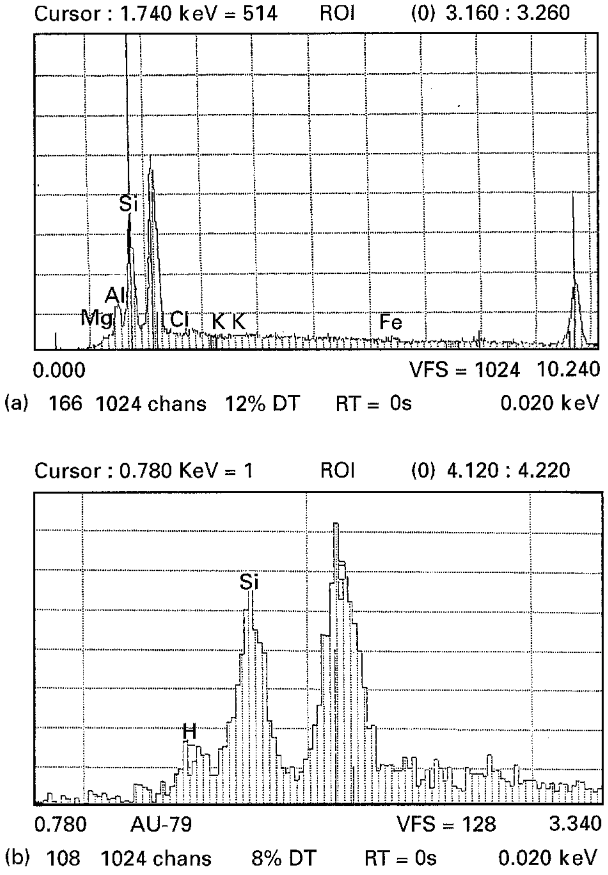

Figure 3 Elemental analysis for SEM of (a) PS–MMT IIIb, and (b) moulded PS–MMT.

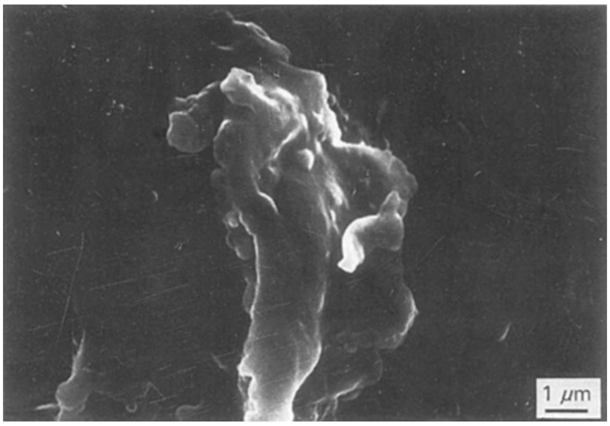

Figure 4 Scaning electron micrograph of PS–MMT IIIb from the unswollen VM–MMT intercalate (× 7800).

Moisture absorption by polymers drastically lowers the glass transition and hence the service temperatures. Thus, the resistance of PS–MMT intercalates to water uptake is a desirable property with these materials. The hydrophilic nature of MMT, which leads to the adsorption of much greater amounts of water molecules, has been changed by its treatment with vinyl cations. This monomer has displaced the second (outer coordination sphere of the cation) and first (primary inner hydration shell) types of the interlayer water that is coordinated to the Na^+ or Ca^{2+} cations in MMT. In addition, the presence of PS chains in the interlayer space has also increased its

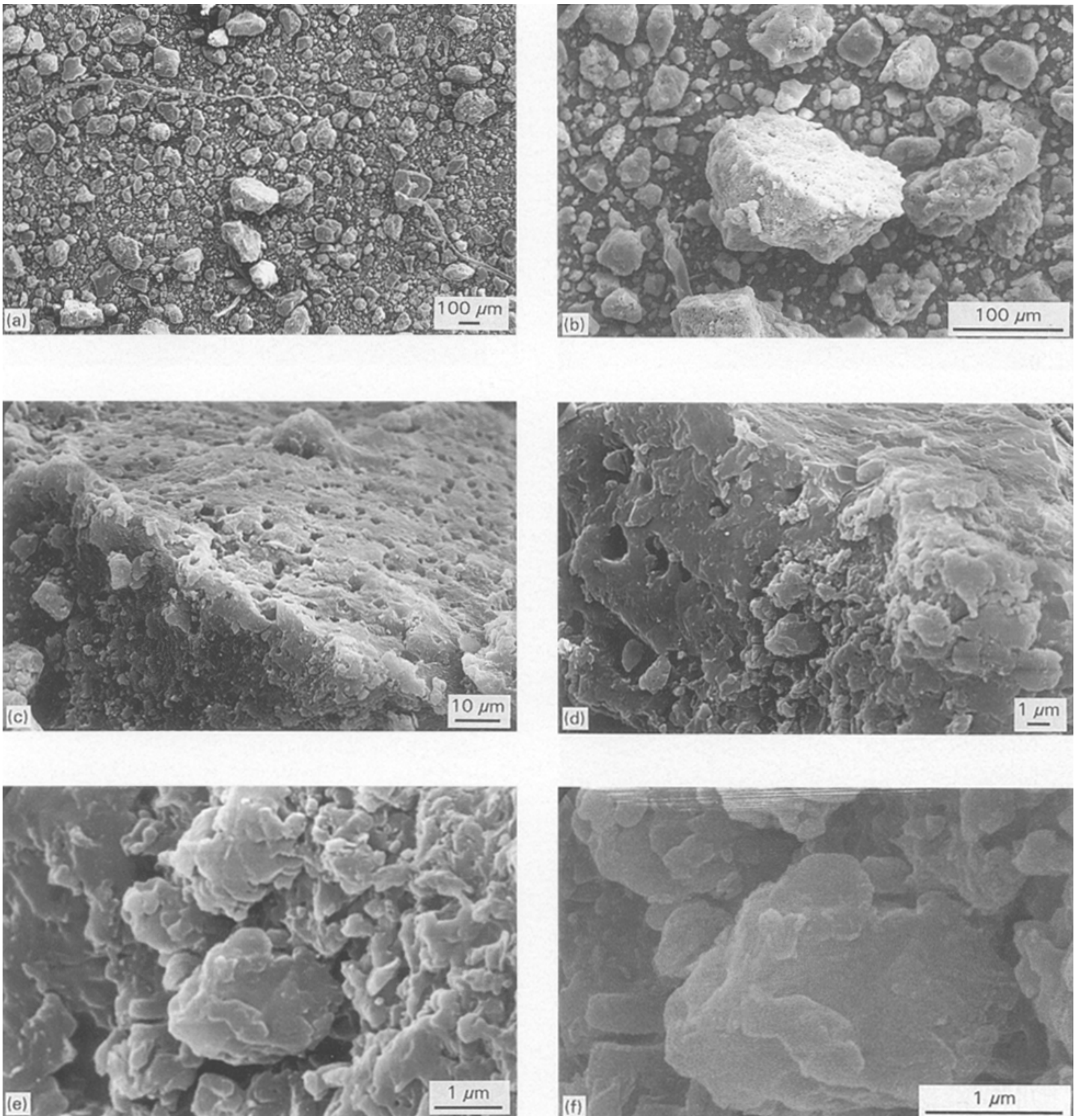

Figure 5 Scanning electron micrograph of PS–MMT IIIb from the pre-swelled VM–MMT intercalate at (a) × 50, (b) × 200, (c) × 1000, (d) × 5000, (e) × 15 000, (f) × 30 000.

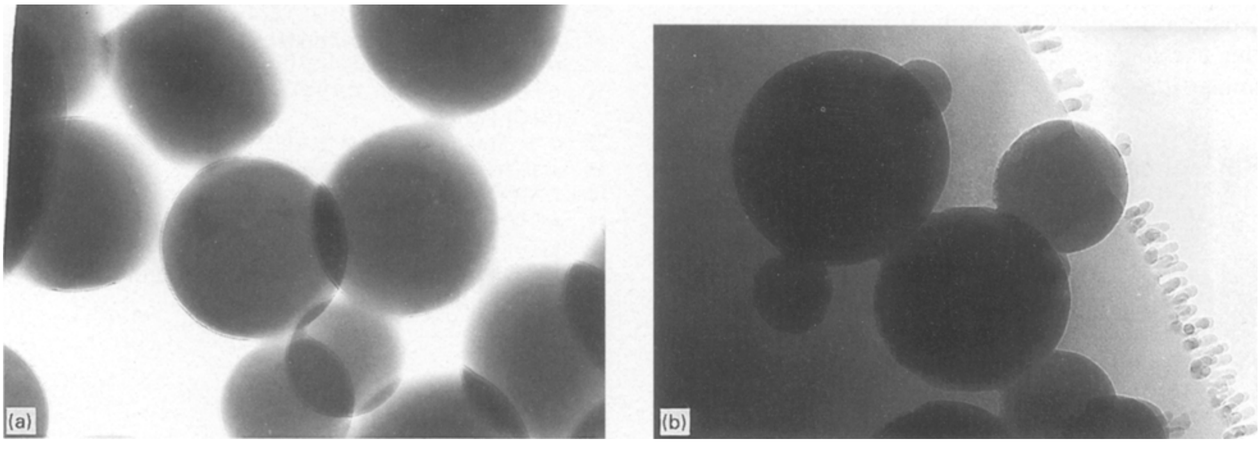

Figure 6 Transmission electron micrograph of PS–MMT IIIb from the pre-swelled VM–MMT intercalate at (a) × 800, (b) × 1000, (c) × 1500, (d) × 2000.

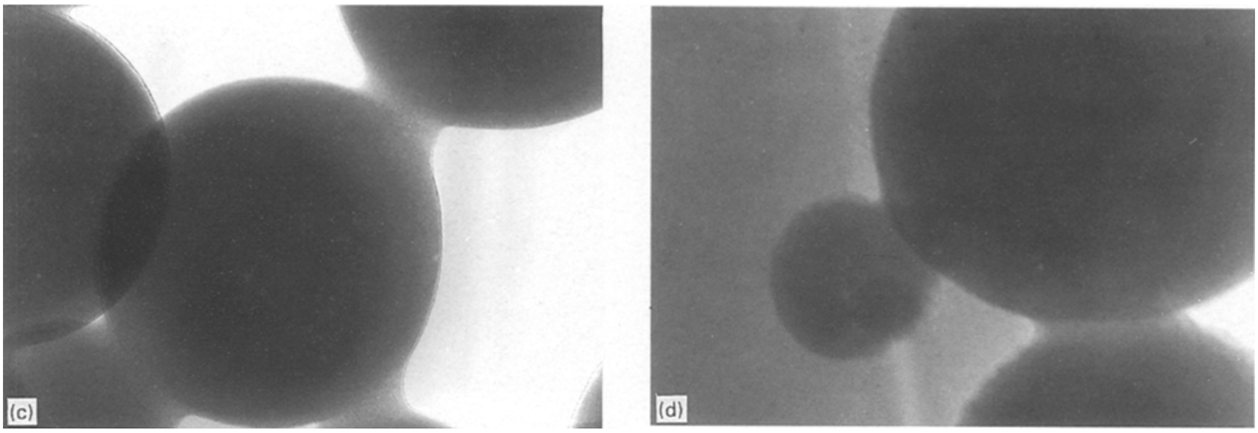

Figure 6 (Continued)

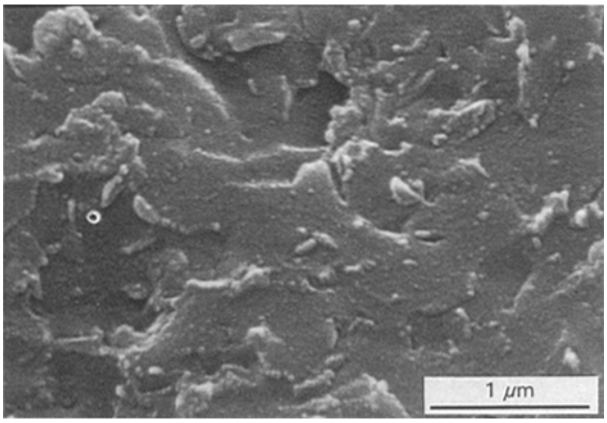

Figure 7 Scanning electron micrograph of moulded PS–MMT, IIIb.

changed behaviour from a hydrophilic to a organophilic nature, due to the chain length and the chemical nature of the PS molecule. These two influences have showed a great reduction in the water uptake capacities of the PS–MMT materials as shown in Table IV. Generally, the exchange reaction of inorganic cations in MMT with organic cations is reversible, i.e. the same equilibrium conditions would be obtained by approach from either side [36]. However, this type of reversible exchange is not realized in these PS–MMT materials when immersed in 0.4 M NaCl solution because the interlayer separation cannot be attained during the course of this exchange reaction, even after about one month immersion.

References

1. B. K. G. THENG, "The Chemistry of Clay–Organic Reactions", (Hilger, London, 1974).
2. B. K. G. THENG, "Formation and Properties of Clay–Polymer Complexes" (Elsevier, Amsterdam, 1979).
3. A. WHEELER, US Pat. 2847391 (1958).
4. H. Z. FRIEDLANDER, *Chem. Eng. News* **42** (6) (1964) 42.
5. H. Z. FRIEDLANDER and C. R. FRINK, *J. Polym. Sci.* **B-2** (1964) 475.
6. A. BLUMSTEIN, *Bull. Soc. Chim. Fr.* (1961) 899.
7. *Idem. J. Polym. Sci.* **A-3** (1965) 2653.
8. R. BLUMSTEIN, A. BLUMSTEIN and K. K. PARIKH, *Appl. Polym. Symp.* **25** (1974) 81.
9. Y. SUGAHARA, S. SATOKAWA, K. KURODA and C. KATO, *Clays Clay Miner.* **36** (1988) 343.
10. F. BERGAYA and F. KOOLI, *Clay Miner.* **26** (1991) 33.
11. C. KATO, K. KURODA and H. TAKAHARA, *Clays Clay Miner.* **29** (1981) 294.
12. H. G. G. DEKKING, *J. Appl. Polym. Sci.* **9** (1965) 1641.
13. *Idem, ibid.* **11** (1967) 23.
14. T. T. GROTENHUIS, US Pat. 2780612 (1957).
15. E. HAUSER, US Pat. 2401348 (1946).
16. *Idem,* US Pat. 2651619 (1953).
17. C. KATO, K. KURODA and M. MISAWA, *Clays Clay Miner.* **27** (1979) 129.
18. Y. FUKUSHIMA and S. INAGAKI, *J. Incl. Phenom.* **5** (1987) 473.
19. Y. FUKUSHIMA, A. OKADA, M. KAWASUMI, T. KURAUCHI and O. KAMIGAITO, *Clay Miner.* **23** (1988) 27.
20. A. USUKI, Y. KOJIMA, M. KAWASUMI, A. OKADA, T. KURAUCHI and O. KAMIGAITO, *Polym. Prepr. ACS Div. Polym.* **31** (1990) 651.
21. D. J. GREENLAND, *J. Colloid Sci.* **18** (1963) 647.
22. C. W. FRANCIS, *Soil Sci.* **115** (1973) 40.
23. R. L. PARFILT and D. J. GREENLAND, *Clay Miner.* **8** (1970) 305.
24. N. SCHAMP and J. HUYLEBROECK, *J. Polym. Sci. Symp.* **42** (1973) 553.
25. E. P. PLUEDDEMANN, "Silane Coupling Agents", 1st and 2nd Edns (Plenum Press, NY, 1982, 1991).
26. E. RUIZ-HITZKY and J. J. FRIPIAT, *Clays Clay Miner.* **24** (1976) 25.
27. A. MOET and A. AKELAH, *Mater. Lett.* **18** (1993) 97.
28. J. E. MULVANCY and D. M. CHANG, *J. Polm. Sci. Polym. Chem. Ed.* **15** (1977) 585.
29. G. D. JONES and S. J. GOETZ, *J. Polym. Sci.* **25** (1957) 201.
30. J. T. CLARKE and A. H. HAMERSCHAG, US Pat. 2780604 (1957).
31. U. HOFMANN, K. ENDEL and D. WILM, *Z. Krist.* **86** (1933) 340.
32. C. E. MARSHALL, *ibid.* **91** (1935) 433.
33. S. B. HENDRICKS, *J. Geol.* **50** (1942) 276.
34. J. MERING, *Trans. Farad. Soc.* **42-B** (1946) 219.
35. A. MATHIEU-SICAUD, J. MERING and I. PERRIN-BONNET, *Bull. Soc. Min. Cristal.* **74** (1951) 439.
36. J. J. FRIPIAT, P. CLOOS and A. PONCELET, *Bull. Soc. Chim. Fr.* (1965) 208.

Received 18 February 1994
and accepted 17 July 1995